Cell Systems, Volume *9*

Supplemental Information

Proteomics-Based Monitoring of Pathway Activity Reveals that Blocking Diacylglycerol Biosynthesis Rescues from Alpha-Synuclein Toxicity

Martin Soste, Konstantina Charmpi, Fabienne Lampert, Juan Atilio Gerez, Marc van Oostrum, Liliana Malinovska, Paul Jonathan Boersema, Natalia Cecilia Prymaczok, Roland Riek, Matthias Peter, Stefano Vanni, Andreas Beyer, and Paola Picotti

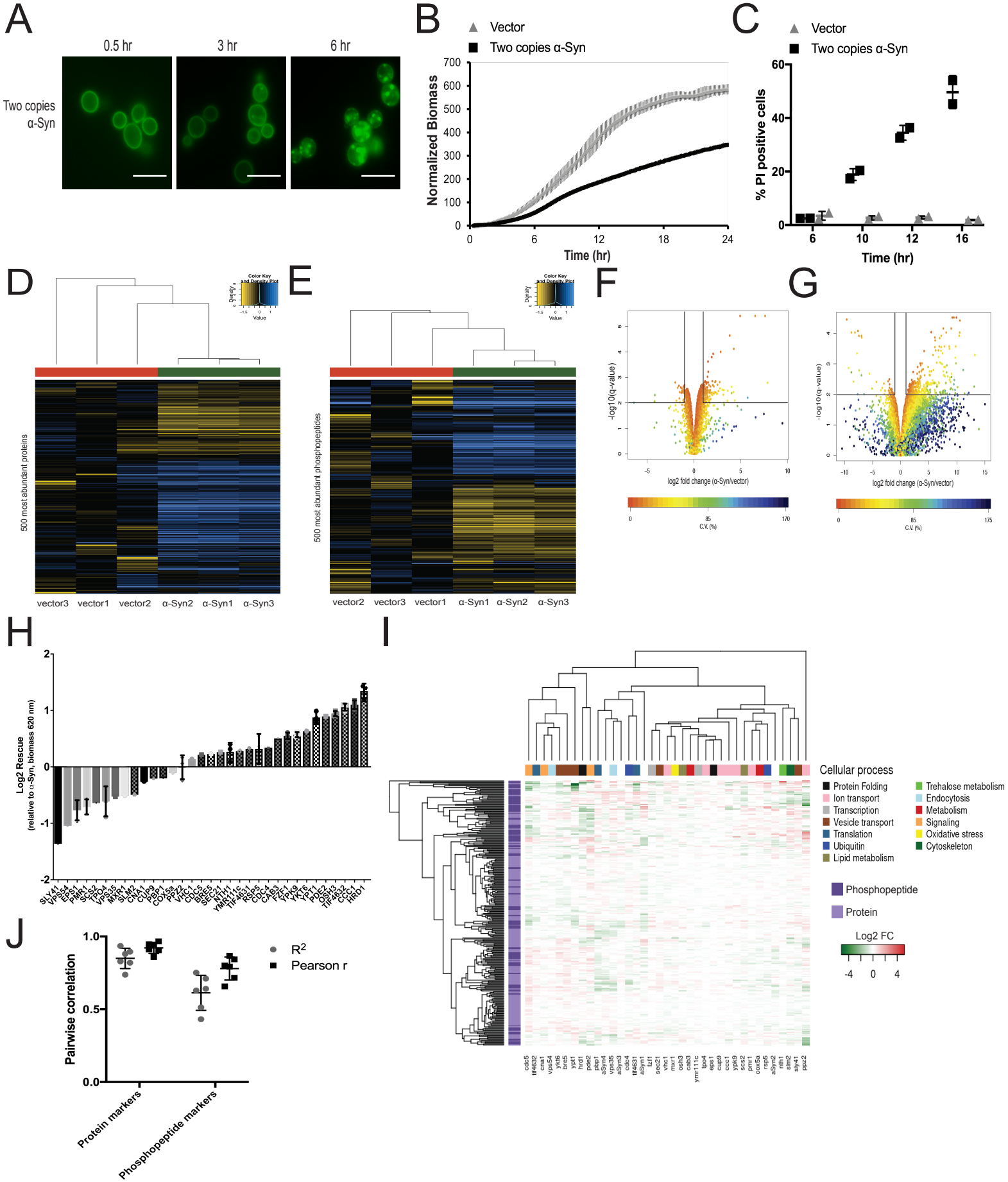

Figure S1. Phenotypic characterization, proteomics and genetic modulation of α-Syn-expressing yeast cells, related to Figure 1, Table S5, STAR methods. The previously described yeast model for α-Syn toxicity (Outeiro and Lindquist, 2003) was assessed **(A)** for the formation of inclusions by fluorescence microscopy of YFP-tagged α-Syn (scale bars represent 10 μm), **(B)** for mean growth inhibition (n=3), and **(C)** for mean cell viability (n=2) relative to vector control. **(D-E)** Hierarchically clustered heatmaps of label-free proteomic quantification displaying the 500 most intense **(D)** proteins and **(E)** phosphopeptides (n=3) **(F-G)** Volcano plots showing significantly regulated **(F)** proteins and **(G)** phosphopeptides in the α-Syn strain relative to vector control. C.V., coefficient of variation. **(H)** Rescue due to overexpression of each modulator calculated relative to growth of the α-Syn-expressing strain without modulation. According to previous studies (see also Table S5), enhancers are shown with solid bars and suppressors with checkered bars. All genes were previously classified as overexpression modulators, except *VPS35* and *COX5a*, which were found to be deletion modulators. Log2 Rescue displayed as mean for modulators analyzed in batches 1-3 (n=3) and as single values for batch 4 (n=1) **(I)** Data from Figure 1B is displayed with clustering by modulator. Modulators are annotated according to their cellular process. **(J)** Mean pairwise correlations (n=6) of sentinel abundances in unmodulated α-Syn-expressing samples from four different proteomic analysis batches. All error bars represent standard deviation.

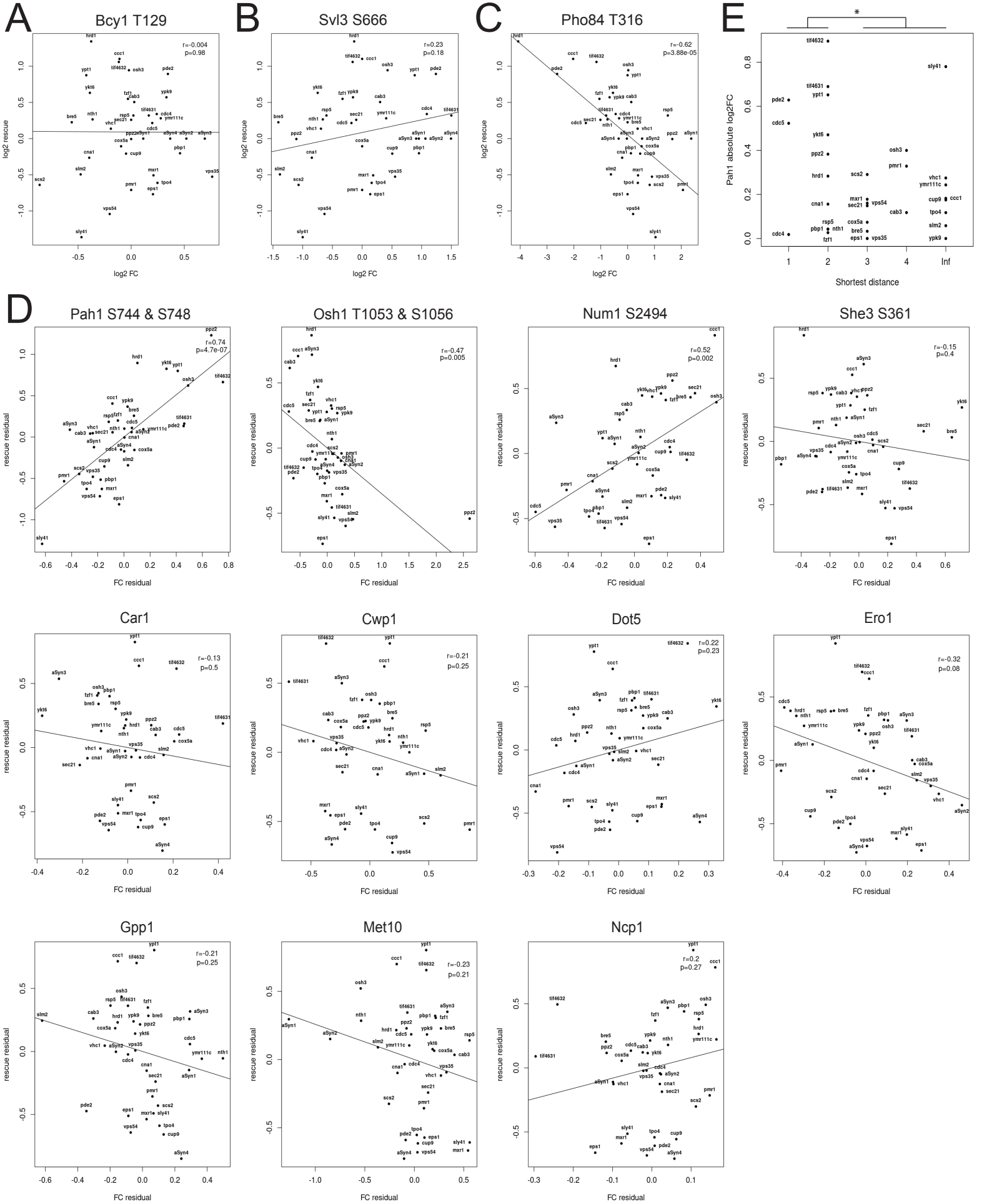

Figure S2. Regression analyses and relationship between Pah1 phosphorylation and modulator distance to the closest Pah1 regulator, related to Figure 1, Figure 2, Table S12 and STAR methods. Additional examples of correlation plots show the extent of rescue plotted as a function of peptide abundance relative to the vector strain. **(A)** Bcy1 T129 is a sentinel for Mck1 kinase activity, PKA and TOR inhibition, and Bcy1 activation (rank 86/103 phosphopeptides). **(B)** Svl3 S666 is an α-Syn deregulated phosphopeptide (rank 95/103 phosphopeptides). **(C)** Pho84 T316 is an α-Syn deregulated phosphopeptide (rank 11/103 phosphopeptides). **(D)** Partial regression is shown for each (phospho)protein sentinel with a maximal selection probability ≥ 0.6. Each panel shows the association of the variables, rescue and abundance, after removing the linear effects of the other sentinels that also passed the stability selection thresholds for both variables. Phosphosites and proteins were treated separately. The best fit line has been added to all plots. r, Pearson correlation coefficient. p, p-value from application of the correlation test (n=37). Note that the residuals are not independent and therefore the degrees of freedom need to be adapted for computing the p-values. **(E)** The log2 fold-change (FC) values of Pah1 S744 and S748 plotted as a function of the shortest path lengths found for the corresponding genetic modulator. If no shortest path was found, the path length was labeled as infinite (Inf). A one-tailed (two-sample) t-test was applied testing if the average FC was greater in observations at distance 1 or 2 (n1=14) compared to observations at distance 3, 4, or Inf (n2=19), *, p-value < 0.05.

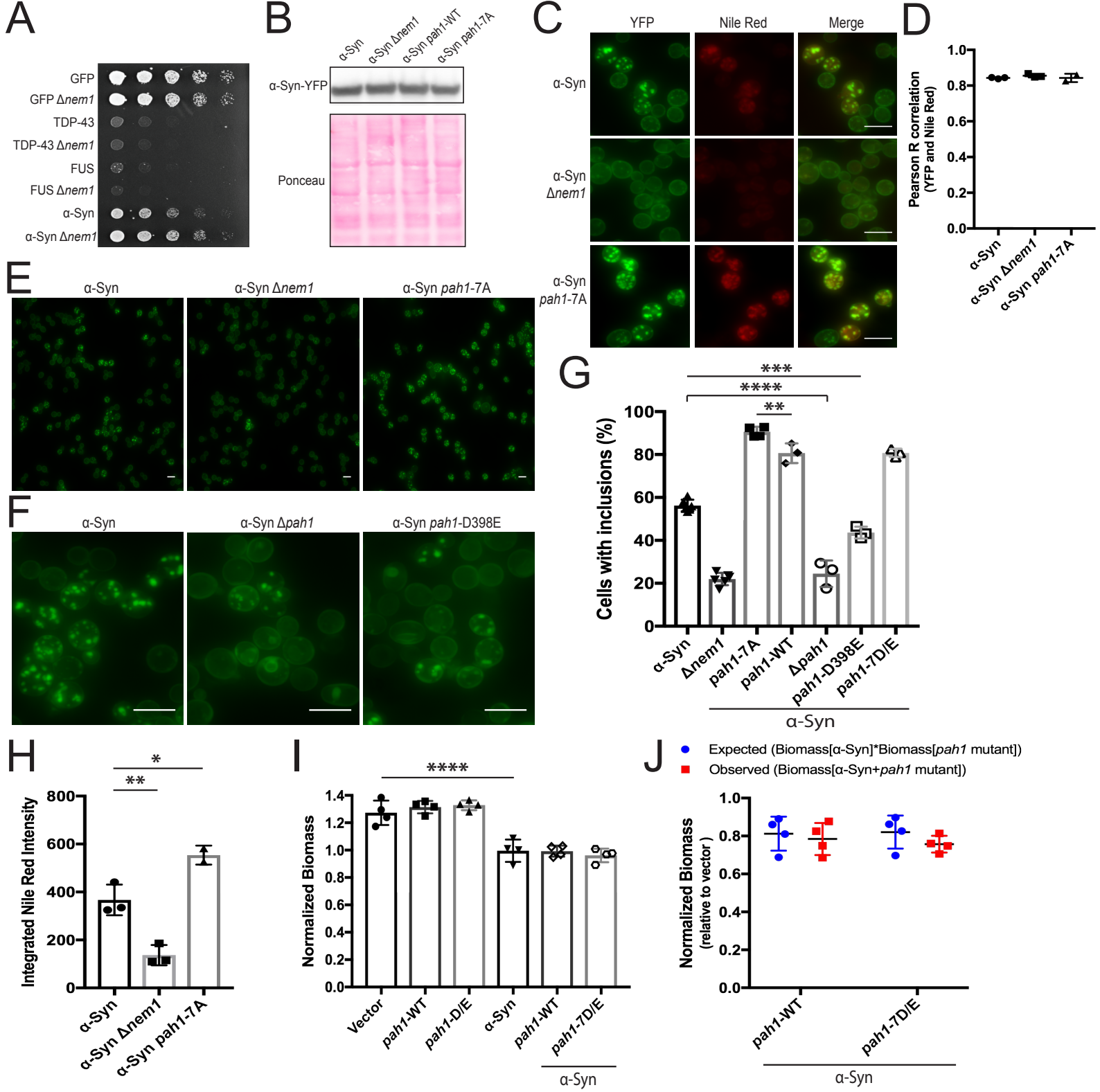

Figure S3. Regulation of α-Syn phenotypes by Pah1 activity, related to Figure 3, Figure 4 & STAR methods. (A) Yeast strains spotted onto galactose-containing medium to induce expression of GFP or other aggregation-prone proteins (n=3) **(B)** α-Syn abundance, assessed by western blot (n=4 for α-Syn and Δ*nem1*, n=1 for α-Syn *pah1*-WT and α-Syn *pah1*-7A) **(C)** Representative images of α-Syn-YFP cells stained with Nile red. **(D)** Co-localization of α-Syn and cellular lipids was assessed by correlation of YFP and Nile red. Mean Pearson R values were compared (one-way ANOVA adjusted for multiple comparisons, n≥2, alpha=0.05). **(E)** Representative fields of view used to quantify the percentage of indicated cells with α-Syn inclusions. **(F)** Representative fields of view of α-Syn-YFP in Pah1 mutants. **(G)** Cells with and without α-Syn-YFP inclusions were counted in three fields of view. Mean counts expressed as percentages with standard deviation between biological replicates for solid data points and between fields of view for hollow data points were compared (n>3 marked with solid data points and n=1 marked with hollow data points; one-way ANOVA adjusted for multiple comparisons, alpha=0.05). **(H)** Mean Integrated Nile Red intensity was used to quantify lipid abundance (one-way ANOVA adjusted for multiple comparisons, n≥2, alpha=0.05). **(I)** Mean normalized biomasses of *pah1*-7D/E mutant or *pah1*-WT yeast strains grown in 1 nM estradiol to induce α-Syn expression were monitored over 24 h (one-way ANOVA adjusted for multiple comparisons, n=4, alpha=0.05) **(J)** Observed and expected biomass of strains expressing α-Syn and a Pah1 mutant. Biomass data from (I) were used and means were compared (two-way ANOVA adjusted for multiple comparisons, alpha=0.05). ****, p-value < 0.0001; ***, p-value < 0.001; **, p-value < 0.01; *, p-value < 0.05. All error bars represent standard deviation. All scale bars represent 10 μm.

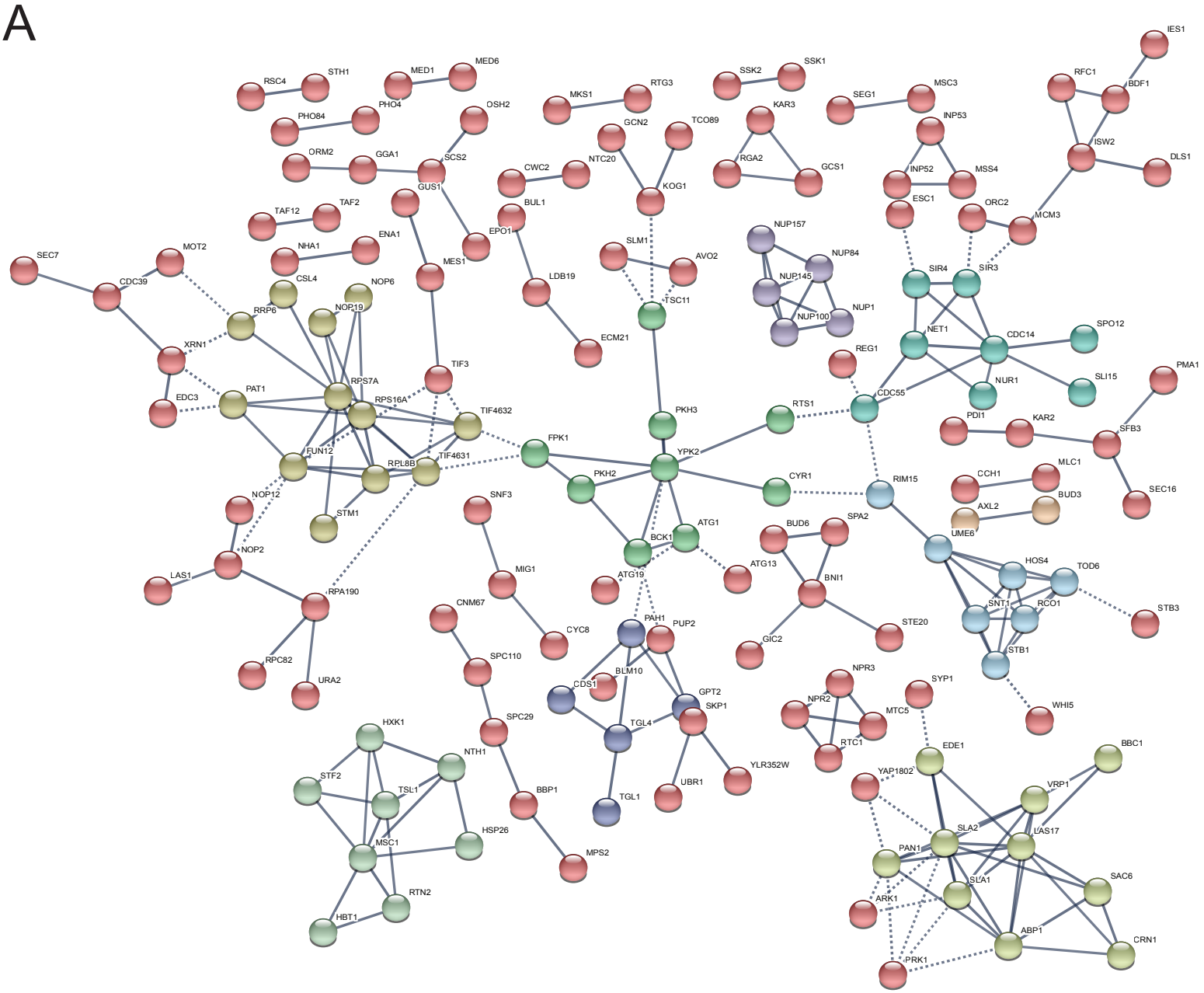

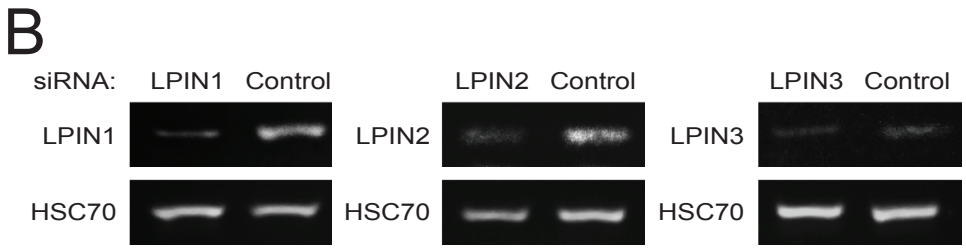

Figure S4. Effects of propranolol on the α-Syn yeast phosphoproteome and siRNA-mediated inhibition of lipins in HEK293 cells perturbed by α-Syn fibrils, related to Figure 4, STAR methods. (A) STRING network of regulated phosphoproteins upon propranolol treatment of estradiol-induced α-Syn yeast. A confidence threshold of 0.9 interaction score was applied. Disconnected nodes were omitted. K-means clustering was set with K=10 and is displayed with different colors. Intra-cluster edges are represented by solid lines and inter-cluster edges are represented by dashed lines. **(B)** siRNA efficiency was assessed by RT-PCR. Cells were transfected with the indicated siRNAs and lipin expression (*LPIN1-3*) was quantified by non-saturating RT-PCR. An unrelated mRNA (*HSC70*) was quantified as a loading control.